Uniform exciton fluorescence from individual self-assembled molecular nanotubes immobilized on solid substrates

Dörthe M. Eisele[1], Jasper Knoester[2*], Stefan Kirstein[1],

Jürgen P. Rabe[1*] and David A. Vanden Bout[3*]

[1]*Humboldt-Universität zu Berlin, Department of Physics, Germany*
[2]*University of Groningen, Center for Theoretical Physics and Zernike Institute for Advanced Materials, The Netherlands*
[3] *University of Texas at Austin, Department of Biochemistry and Chemistry, USA*

Corresponding authors:
j.knoester@rug.nl, rabe@physik.hu-berlin.de , dvandenbout@cm.utexas.edu,

Supplementary material contains:

i. Immobilized J-aggregates on Solid Substrates

Figure S_1a displays a representative SFM image of J-aggregates deposited on quartz surfaces by traditional *spin-coating*. This preparation method produced heterogeneous coverage on the slide with some regions having a high density of aggregates and others showing almost no aggregates. The aggregates form a network of bundles of various thicknesses and lengths of several microns that cross each other rather than merging into large bundles.

Since the optical properties of the tubular J-aggregates strongly depend on their specific supramolecular structure, the absorption and emission spectra from the sample can be used to determine if the molecular structure of the aggregates has changed upon deposition onto the substrate. Because the tubules on the substrate are highly dilute, emission spectra rather than the very weak absorption spectra were used. Emission spectra were collected rather than excitation spectra because of the extremely small Stokes shift for the emission.

Figure S_1b compares the emission spectra of J-aggregates prepared on quartz substrates via the traditional *spin-coating* as compared to the solution spectrum. The sample exhibits clear differences with respect to the solution concerning energy and particularly the width of the peaks. **Figure S_1c** also shows that J-aggregates prepared via the *drop-flow technique* and dried on the surface by blowing with nitrogen clearly changed their structure: the aggregate peaks are broadened and the ratio of the peak intensity changed compared to the solution.
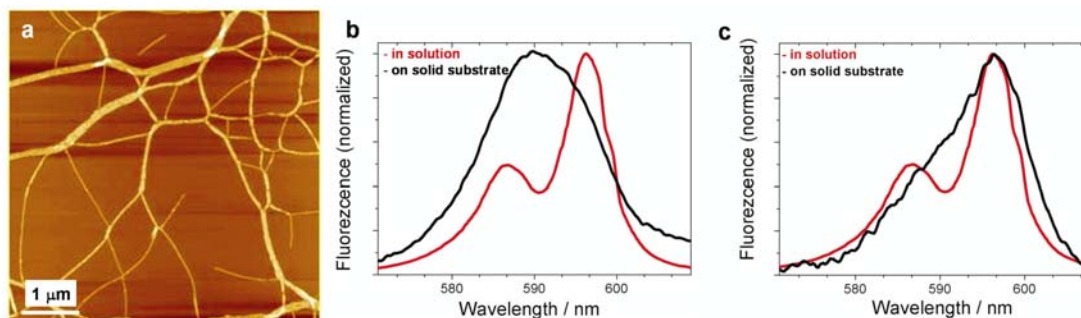
Figure S_1: (a) SFM Images (tapping mode) of tubular J-aggregates on a quartz surface prepared via traditional *spin-coating* yields a non-homogeneous sample with mostly intertwined aggregates. **(b)** Emission spectra of tubular J-aggregates in solution (red) and after preparation on a quartz surface (black) via *spin-coating* and slowly drying in air **(c)** Idem, but now the black line is the spectrum of aggregates prepared on quartz via the *drop flow technique* and drying by blowing with nitrogen.

As shown in the manuscript, the sample prepared by the *drop-flow technique* and carefully dried in air in a black box had spectra that were nearly identical in both position and width to the solution, indicating no significant morphological and structural changes upon deposition.

ii. SFM line scans
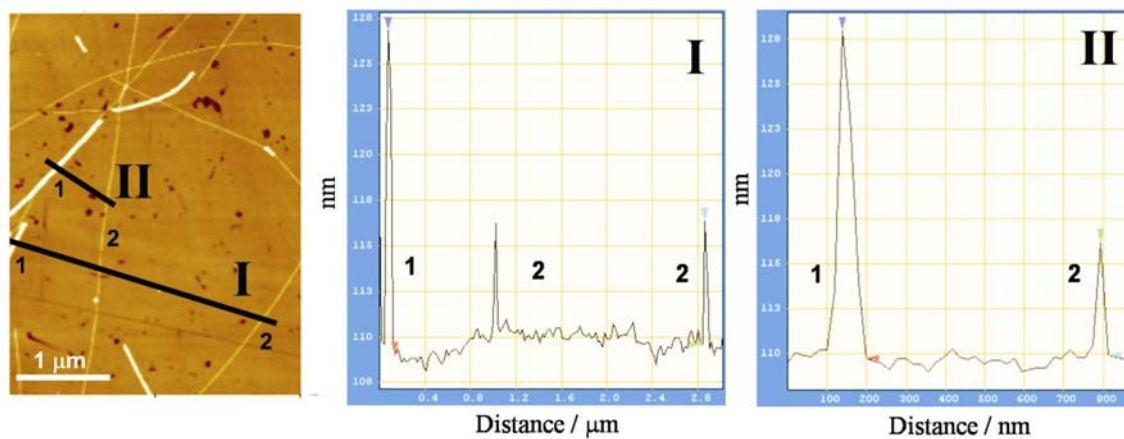
**Figure S_2:** (a) Scanning force microscopy image of tubular J-aggregates immobilized on a quartz substrate. Long nanostructures with distinct heights (18 ± 2) nm (**1**) and (6 ± 1) nm (**2**), are clearly visible (see line scans in I, II). The thinnest objects are attributed to single tubular aggregates and the thicker ones to bundles of such aggregates.

iii. Optical resolution, NSOM images line scans
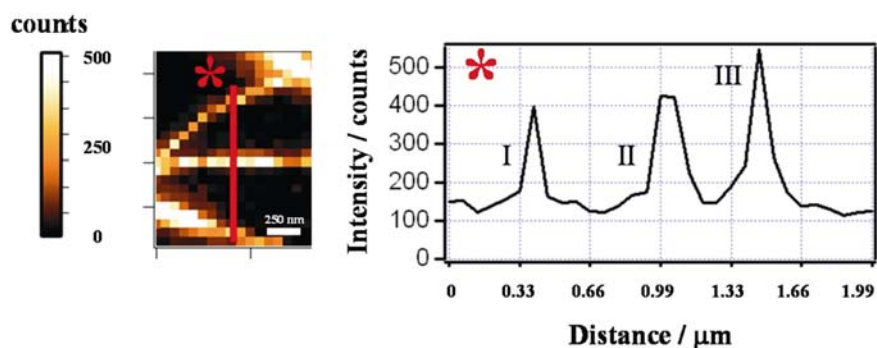

Figure S_3: Optical Resolution of Emission NSOM. Tubular J-aggregates on glass surface; section of a fluorescence NSOM image. The dwell time at each pixel was 40 ms; line scan on the total emission image is marked with (*), which shows that the optical resolution of ~ 70 nm [FWHM of the objects in the line scans I (43±3) nm; II: (77±6) nm; III (59±4) nm].
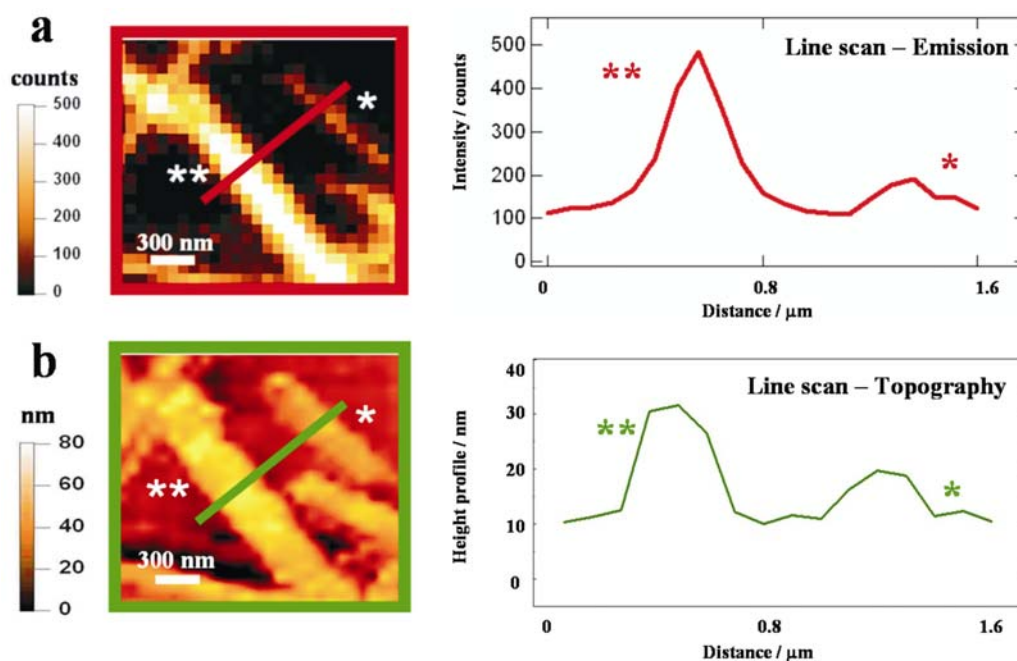
Figure S_4: Single tubes and bundled tubes are distinguishable. The emission (a) corresponds to the topography (b) of a NSOM scan of tubular J-aggregates on a glass substrate. Single tubes (*) and bundled tubes (**) can be distinguished by their emission intensity in the emission image and by their different heights in the topography image. (c) Line scans on the emission image (red) and on the topography image (green) show a bundled tube (**) and a single tube (*).

The NSOM fluorescence and topography images in figure S_4 are acquired simultaneously, which allows the fluorescence intensity to be correlated with the object height. The object marked with (*) has the smallest height and emission intensity of any object found in the image. The line scan that has been taken over (*) reveals an apparent height of $*_{(7\pm2)}$ nm, and emission intensity of $*_{(200\pm15)}$ counts. Analysis of the background regions free of tubes reveals the background has a count rate of $_{(120\pm11)}$ counts. This yields an intensity of on average 80 counts for the smaller object identified as a single tube. The apparent height values for the larger object marked with (**), (22 ± 2) nm. As with the SFM images there is an offset in the height of about 6 nm. This makes the height of the single tube 13 nm and the bundle 28. The bundles are approximately twice as tall as single tubes. The emission intensity for the larger object marked with (**), (500 ± 23) counts. Removing the background yields an average fluorescence 380 counts which is approximately four to five times the values for the single tube. The bundles are likely two by two stacks of individual tubes.
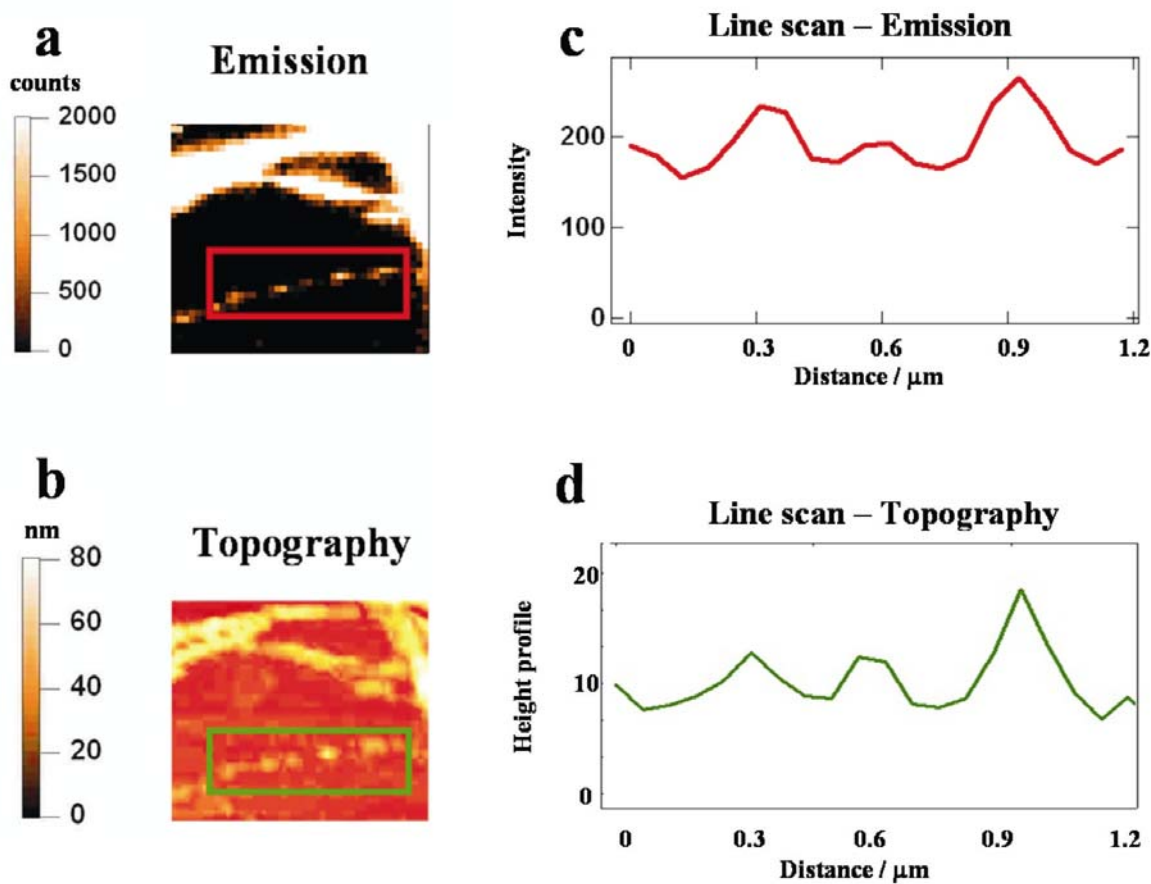
Figure S_5: Tubes with non-uniform fluorescence could be identified as broken tubes. (a) Fluorescence NSOM image showing broken aggregates. **(b)** The corresponding topography image. **(c)** Line scan of the fluorescence for the aggregate highlighted in the box in the emission image. **(d)** Corresponding topography line scan.

Figure S_5a shows an example of a tube which exhibits large variations in the fluorescence intensity along its length. The corresponding topographic image (**figure S_5b**) reveals that this aggregate does not have a uniform morphology but has been broken, most likely upon deposition. Similarly, the majority of other tubes can be identified as being morphologically intact single tubular aggregates.
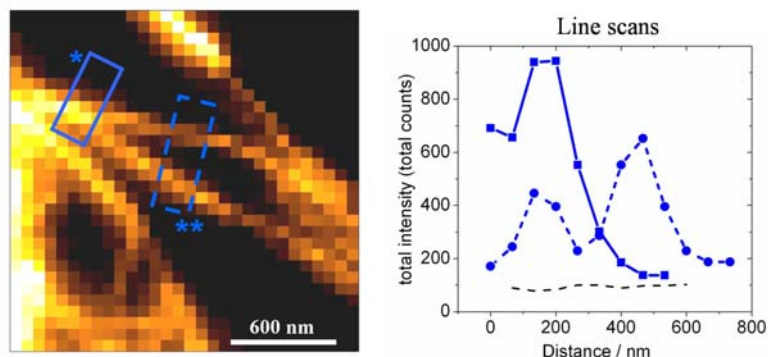
Figure S_6: Individual tubes merging into bundles Fluorescence NSOM image of aggregates (**)that merge into a bundled aggregate (*). Line scans perpendicular to the aggregates on (a) averaging over 200 nm. The ratio of the total intensities of the bundled aggregate (*) and of the sum of the total intensity of the two separated aggregates (**) is 0.93 ± 0.08 indicating no significant quenching of the fluorescence in the bundled aggregates.

Different representative example (than given in the main text) of the fluorescence image of aggregates that merge into a bundled aggregate; line scans perpendicular to the aggregates on the image averaging over 200 nm. The ratio of the total intensities of the bundled aggregate (**) and of the sum of the total intensity of the two separated aggregates (*) is 0.93 ± 0.08, indicating no significant quenching of the fluorescence in the bundled aggregates. This can be explained by the fact that the main part of the total fluorescence intensity can be attributed to the inner wall. Thus the outer wall is contributing only little to the total intensity and is protecting the inner wall against quenching.

iv. Fluorescence of morphologically intact single tubes

As the NSOM image in **figure S_7** is collected on a pixel-by-pixel basis, the fluorescence of intact tubes is not perfectly constant at each point in the line scan along a single tube. Therefore the question arises:

Do the intensity fluctuations along a tube result from non-uniform optical properties or only from the statistical fluctuations of the photon counting process?

First, the background in **figure S_7a** has been carefully investigated, where no tubes or other objects could be identified in the topography image. A representative example for a background sample is shown in **figure S_7b,** where the background consists of 100 data points. The mean value is 116.6 counts (**table S_1**).

Mean signal $\bar{x}$	$\bar{x} = 116.6 \, \text{counts}$	$\bar{x} = \dfrac{1}{N-1}\displaystyle\sum_{j=1}^{N} x_j$
Standard deviation Δx of $\bar{x}$	$\Delta x = \pm 10.7 \, \text{counts}$	$\Delta \bar{x} = \sqrt{\dfrac{1}{N-1}\displaystyle\sum_{j=1}^{N}(\bar{x} - x_j)^2}$
Standard deviation σ of Poisson distributed sample	$\sigma = \pm 10.7$	$\sigma = \sqrt{\bar{x}}$

Table S_1: Data taken from the background example sample shown in **figure S_7**

Based on photon counting statistics one would expect the standard deviation of this sample to be the square root of the mean, or 10.7 counts. The normal standard deviation of the background was found to be 10.7 counts (**table S_1**) indicating that the fluctuations are indeed shot-noise limited.

Emission

10 pixel x10 pixel = 100 data points
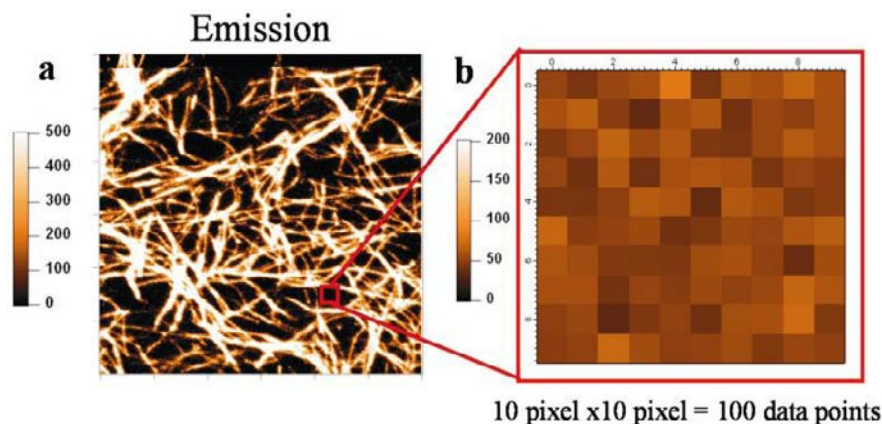
Figure S_7: (**a**) Total fluorescence image of aggregate sample. (**b**) Zoom of a small region that contains no aggregates. The emission from this region was analyzed to examine the fluctuations in the background signal.

The tube's emission has been characterized with line scans along segments of single tubes in the NSOM emission image displayed in **figures S_7a.**

Tube segments have been chosen from tubes that

    a) can be identified in the topographic image as morphologically intact tubes in the corresponding topography image displayed,

    b) are well separated from others, as compared to the optical resolution,

    c) are lying straight (no curves) on the surface over a certain distance,

    d) have a comparable background along the length of the tube segment,

    e) exhibit segments that are longer than about 270 nm, i.e. they have more than 4 pixels (data points y_j with $j > 4$, where 1 pixel = 66.7 nm).

v. Statistical analysis of tube's fluorescence

Assuming that the fluorescence from the tubes is spatially uniform, the fluctuations in the line scan should only result from the photon counting statistics. This will lead to a Poisson distribution of the data y_j. Assuming the samples y_j come from a Poisson distribution (null hypothesis H_0), the appropriate index of dispersion for small sample numbers that are Poisson distributed is the statistic[1]

$$x^2 = \sum_j (y_j - \overline{y})^2 / \overline{y} \qquad \text{(B1)}.$$

In case the sample follows the assumed distribution then there is a probability α to get the value χ^2_{df}, which is larger or equal to the determined value x^2. The tubes will have uniform fluorescence along the long axis if the determined value x^2 yields a value χ^2_{df}, for which $P(\chi^2_{df} \geq x^2) > 5\%$. Based on the null hypothesis H_0 that all the y_j come from the same Poisson distribution, the sampling distribution of x^2 is χ^2_{df} on df degrees of freedom, and the significance level of x^2 with respect to this hypothesis is $P(\chi^2 \geq x^2) > 5\%$ in "significant agreement" with the assumed distribution. The above test has been used to investigate the statistical signal fluctuations along single tube segments. Results have been listed in **table S_2**. In all cases it is impossible to distinguish the photon statistics for the measured samples from the expected Poisson distribution.

df = N - 1	6	10	5	11	13	6	4	10	3
$x^2 = \sum_j (x_j - \overline{x})^2 / \overline{x}$	1.61	4.61	0.82	3.28	5.28	4.69	0.4	5.32	1.14
$P(\chi^2_{df} \geq x^2) = \alpha$	95%	90%	95%	98%	95%	50%	98%	80%	80%

Table S_2: Values α taken from the table of the Percentage Points χ^2_{df} of the Chi-Squared Distribution for which $P(\chi^2 \geq x^2)$ is true.

---

[1] Ledermann,W. Handbook of applicable Mathematics VIb (1986)

vi. Emission dichroism data and error determination

The reduced linear dichroism, D, has been determined for a number of individual J-aggregates immobilized on a solid substrate. For each single aggregate, the angle Φ of the tube relative to the polarizer (scan direction or image frame), was determined by identifying straight segments of single aggregates and determining their orientation from the coordinates of the ends of the segments. The error in each data point is dependent on the length of the segment, with longer segments yielding more accurate angles.

The average fluorescence intensity of each segment was calculated by taking a line along identical segments in each of the polarized images. The error of each data point was determined from the shot noise of the fluorescence signal.

vii. Exciton transport length in individual double walled nanotubes

In the following the two estimates of the exciton transport length given in the paper will be explained. They represent the limits of coherent and incoherent (diffusive) transport, which lead, respectively, to upper and lower bounds for the transport length.

For coherent transport the jump time between two molecules is given by the inverse of the typical intermolecular excitation transfer interaction, which depends on the geometry of the system. Here we use the geometry model from previous work on a similar system,[1] which gives typical interaction strengths with a magnitude of the order $J = 300\,cm^{-1}$. Also the red-shift of the J-bands relative to the single-molecule transition observed by us is indicative of this typical interaction strength. From this we obtain a jump time of $\frac{1}{J \cdot 3 \cdot 10^{10}}s = 100\,fs$. The lifetime τ of the excitations on the inner tube we can take to be of the order of 100 ps.[2] This results in the possibility of 1000 jumps as the upper limit for exciton transport. Taking 1 nm as typical molecular dimensions, we thus obtain a maximum transport length of L_{coh}=1 μm. Probably this upper limit overestimates the actual value, as coherent transport over such distances is unlikely at room temperature.

The other extreme is obtained by assuming that all transport between neighboring molecules occurs through incoherent Förster transfer: the jump rate between molecules is then of the order of J^2/Γ, where Γ is the typical homogeneous line width of the exciton transitions.[3] Given that the total line width of the low-energy J-bands is approximately 300 cm^{-1}, the estimate for the jump time in the Förster limit now also amounts to about 100 fs. We have to keep in mind, however, that this now refers to diffusive motion. The diffusion constant D is given by the square of the intermolecular distance, divided by the jump time, which leads to $D = 1$ nm^2 / 10^{-13} s $= 0.1$ cm^2/s. The diffusion length then would be $L_{diff} = \sqrt{D\tau} = 30\,nm$.

References for Supplementary Information

[1] C. Didraga, A. Pugzlys, P. R. Hania, H. von Berlepsch, K. Duppen, and J. Knoester, Structure, spectroscopy, and microscopic model of tubular carbocyanine dye aggregates J. Phys. Chem. B **108** (39), 14976-14985 (2004).

[2] A. Pugzlys, R. Augulis, P. H. M. van Loosdrecht, C. Didraga, V.A. Malyshev, and J. Knoester Temperature-dependent relaxation of excitons in tubular molecular aggregates: fluorescence decay and Stokes shift. *J. Phys. Chem. B* **110**, 20268-20276 (2006).

[3] P. Reineker. *Exciton Dynamics in Molecular Crystals and Aggregates,* G. Höhler, Editor, Springer Tracts in Modern Physics 94, Springer-Verlag, Berlin (1982).